INDONESIAN JOURNAL ON GEOSCIENCE
Geological Agency
Ministry of Energy and Mineral Resources

Journal homepage: http://ijog.geologi.esdm.go.id
ISSN 2355-9314, e-ISSN 2355-9306

Geophysical Investigation of Buried Small Fault Beneath Western Mount Malabar Using Electrical Resistivity Tomography in The Great Bandung Basin Rim

Kusnahadi Susanto[1], Asep Harja[1], Farham Rezqi Ma'arif[2], and Husneni Mukhtar[3]

[1]Department of Geophysics, Universitas Padjadjaran, Bandung, Indonesia
[2]Geophysics Study Program, Universitas Padjadjaran, Bandung, Indonesia
[3]School of Electrical Engineering, Telkom University, Bandung, Indonesia

Corresponding author: k.susanto@unpad.ac.id
Manuscript received: February 15, 2024; revised: June, 28, 2024;
approved: September, 27, 2024; available online: December, 6, 2024

Abstract - This article presents the discovery of a buried fault beneath the soil layers in the Mt Malabar area, which complements the information on suspected faults on the previous geological maps. Using an Electrical Resistivity Tomography (ERT) method, this study aims to delineate the layer discontinuity as a fault and describe the subsurface geology. This study employed a 1400 m long ERT line as the main line to identify buried fault traces, while each ERT line has an 800 m long installation across the main ERT line to obtain the direction of the minor fault. The investigation found a minor fault in the rock layer at a high resistivity layer, approximately 160 m below the surface. The identified rock units are believed to include sandy clay in the upper layer, followed by tuff, sandstone, and basalt lava in the lower layer because its resistivity value is above 250 Ohm.m. The 3D ERT model interpreted a minor buried fault as a weak zone beneath the soil and obtained the fault strike at approximately N 310°E and dipping 66°. Furthermore, these results are strengthened by the geological map, which confirms that ERT L-1 and ERT L-3 profiles coincide with a suspected fault in the Qmt rock unit area.

Keywords: minor buried fault, electrical resistivity tomography, Mount Malabar, 3D model

How to cite this article:
Susanto, K., Harja, A., Ma'arif, F.R., and Mukhtar, H., 2024. Geophysical Investigation of Buried Small Fault Beneath Western Mount Malabar Using Electrical Resistivity Tomography in The Great Bandung Basin Rim. *Indonesian Journal on Geoscience*, 11 (3), p.409-421. DOI: 10.17014/ ijog.11.3.409-421

Introduction

Mount Malabar, located in southern Bandung, features a complex geological setting, primarily composed of volcanic rocks formed by past volcanic activity. The area has several minor buried faults, significantly influencing the Bandung region southern rim. The geological map indicates many minor buried faults on the southern rim of the Bandung Basin (Alzwar *et al*., 1992). To accurately identify and characterize these buried fault systems, a method must be used to investigate their existence.

A nondrilling way to estimate subsurface characterization is to apply geophysical techniques such as geo-electric and seismic methods (Rey *et al*., 2020). This method is used if faults buried in the ground have been indicated first. Next, drilling techniques are considered after obtaining more definite information.

The use of geo-electric methods to investigate buried faults has been widely used in several case studies, such as in a fault zone located in the southwestern part of İzmir City, where the fault creeps in the urban area of San Gregorio in Catania, the southern flank of Mount Etna, Sicily - Italy (Drahor and Berge, 2017; Imposa *et al*., 2015), or in the southern Apennines and St. James (Galli *et al*., 2006; Jacob *et al*., 2013; Imposa *et al*., 2015). Although the geophysical methods encounter a significant restriction in measurement resolution, their interpretation can be ensured to be accurate by performing a specific validation procedure, such as well testing.

This paper outlines a geophysical exploration of a minor fault within the volcanic zone of Mount Malabar. This mount is located in the Great Bandung Basin with the highest peak reaching 2,968 m. The mountain surrounding the Greater Bandung Basin has several faults due to the subduction zone slab movement activity in the southern part of the Java Island (Harja *et al.*, 2021). Mount Malabar has a complex volcanic history characterized by the evidence of various geomorphologic processes lasting more than 50,000 years (Dam *et al.*, 1996). Mount Malabar is a stratovolcano composed of layers of lava, pyroclastic material, and volcanic ash formed by successive eruptions over time (Dam *et al.*, 1996; Haryanto *et al.*, 2017).

Mount Malabar has been an intriguing research object in geoscience studies, especially hydrological research disasters and geothermal energy resources. Many studies have been conducted on geophysical, geological, and geochemical methods around Mount Malabar (Sudarman *et al*., 2006; Handayani *et al*., 2012a; Haryanto *et al*., 2017). One of them uses the gravity method. Handayani *et al*. (2012b) stated that using gravity could indicate a possible active fault.

The Electrical Resistivity Tomography (ERT) method is a powerful and cost-effective geophysical method that can detect buried faults in urban areas, can determine the thicknesses of soil and basalt flows, and can identify other subsurface geological structures (Storz *et al*., 2000; Al-Amoush and Rajab, 2018; Susanto *et al.*, 2023). The ERT survey can traverse the electrodes along a straight line or create a grid to cover a larger area. To address the problem of a larger studied area and monitoring, several studies have developed an automatic resistivity meter with an optimized data acquisition protocol and remote operation to servers using a wireless internet connection or a Long-Range Radio (LoRa) communication with the advantage of low-power communication (Binley and Slater, 2020; Qiang *et al*., 2022; Nurpadillah *et al.*, 2024; Holmes *et al.*, 2020). However, automatic and remote operation is not yet needed to investigate the buried minor faults in western Mount Malabar unless the study aims to detect the water reservoirs.

ERT provides fast and low-cost 2D and 3D subsurface models compared to other geophysical methods such as seismic and deep well-tests fields (Griffiths and Barker, 1993; Epting *et al*., 2012; Drahor and Berge, 2017). ERT is also used to discover a minor fault buried due to volcanic activity in a past event and buried through erosion, weathering, and other climate processes. Discontinuities in rock layers were due to active fault deformation in Ambon, which triggered some land subsidence in Negeri Sila, Nusalaut, and Central Maluku (Amukti *et al*., 2022), which were reported using ERT. Furthermore, the other use of ERT was for the identification of lateral changes in facies and minor faults at Loma de Ubeda, southeastern Spain (Rey *et al*., 2020), and fault network formation in the Callovo-Oxfordian black marls, such as Super-Sauze big landslide and Draix-Lava Landslides (Marc *et al.*, 2017).

The purpose of this study is to investigate minor or shallow buried faults around the slopes of Mount Malabar using the ERT method. This study can advance our understanding of the geological conditions in the relatively shallow subsurface, especially the minor faults, and can recognize geological structures in various geological fields, such as rain catchment areas, areas with potential geological disasters, and natural resource prospect areas (Saputra *et al.*, 2020; Fronzi *et al.*, 2021).

Studied Site

Mount Malabar is a volcanic complex in the southern Bandung Basin rim of West Java, Indonesia. As a Quaternary volcano, Mount Malabar is the central structure in the southern part of the Bandung Basin. The Malabar Volcanic Complex was formed during the Pleistocene era (Dam *et al.*, 1996; Bogie *et al.*, 1998; Hendarmawan, 2002). Mount Malabar is a stratovolcano with volcanic rock layers such as lava, tuff, and breccia (Bronto, 2006). The rock consists of andesite, basalt, and pumice. Brown volcanic ash forms the matrix with poor sorting. Furthermore, rock unit descriptions have been comprehensively described in the southern Bandung region geological disaster potential and prospect zone (Sulaksana *et al.*, 2019). Mount Malabar is encircled by a complex alluvial system that primarily flows towards the Bandung Basin. Substantial evidence indicates the presence of numerous steep slope gradients on the northern aspect of Mount Malabar, oriented towards the Bandung Basin (Suhari and Siebenhüner, 1993; Pratama *et al.*, 2016). Figure 1 illustrates Mount Malabar position in the Bandung Basin.

Geophysical measurements were conducted on the northern (7° 3' 35.89" S and 107° 38' 45.83" E) and western slopes (7° 8' 10.91" S and 107° 36' 35.66" E), with slope gradients mainly in the range of 25 - 45 %. The peak of Mount Malabar is at 2,968 m above sea level (m asl.), while the studied area is located on the western slope of Mount Malabar, approximately 1400 m asl. The erosion process around Mount Malabar is cone-shaped volcanoes giving rise to an intricate alluvial system. Due to the prevailing circumstances, the minor faults have become increasingly obscured and are likely to be buried beneath the surface terrain. A blue box in Figure 2 shows the geological map of minor faults buried in the Qmt rock unit area. In addition, the thin weathering layer in the studied area indicated that ground movement rarely occurred. Thus, natural disasters like landslides and debris flows are rare near Mount Malabar (Harja *et al.*, 2021).

The studied area is rich in water springs that emerge from cracks in the volcanic rocks. However, at the base of Mount Malabar, the water supply is limited, possibly due to faults that intersect the aquifer. In addition to springs, several streams traverse the area. Other characteristics include rock outcrops, although these do not offer definitive information on the minor faults under investigation.

Methods and Materials

Methods

Electrical resistivity tomography (ERT) is a geophysical method that can detect minor buried faults. In general, ERT can be a helpful tool for

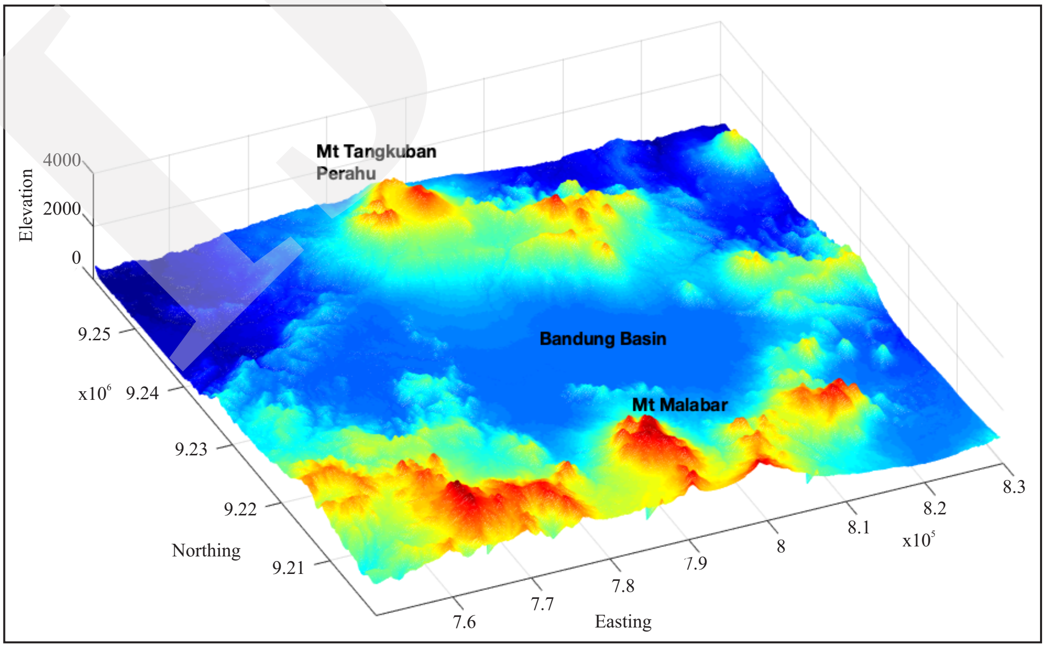

Figure 1. The digital elevation model of the Great Bandung Basin and Mount. Malabar as the studied site.

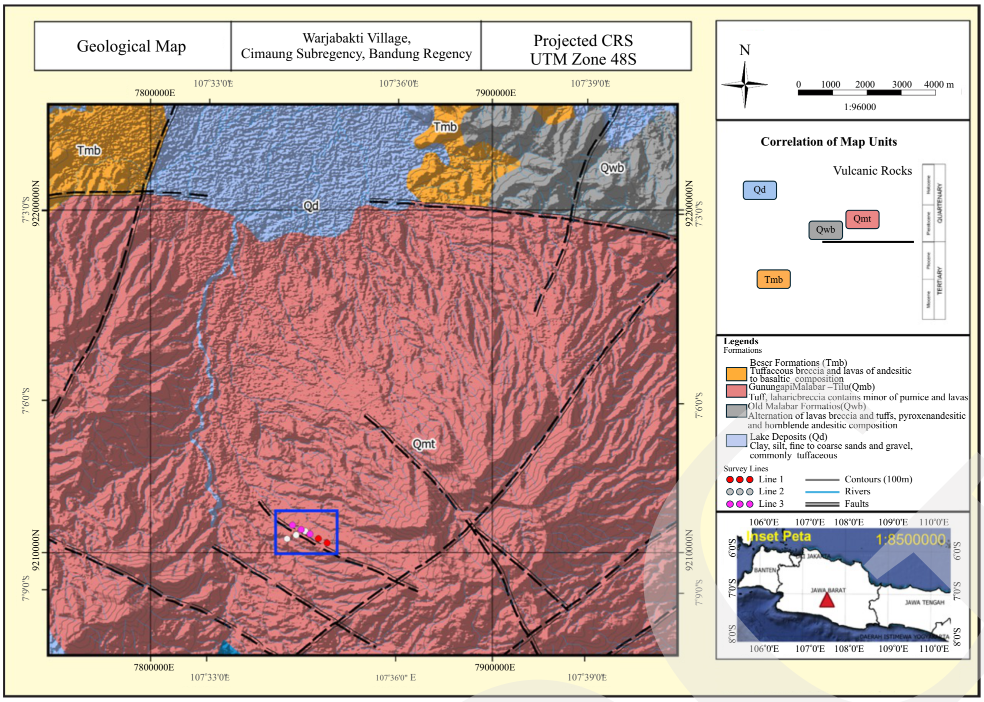

Figure 2. Geological map of the studied area. The studied site is Qmt unit rock, consisting of tuff, breccia, basaltic lava, and pumice (Source: Alzwar *et al*., 1992, BIG).

detecting minor buried faults, providing high-resolution images of the subsurface, and allowing for the identification of geological structures and changes in lithology. The electrodes inject electrical current into the ground, resulting in voltage being measured. Based on the electrical properties of the subsurface materials, ERT can provide a three-dimensional image of the subsurface, traversing the electrodes along a straight line or creating a grid to cover a larger area. The electrode number and spacing may vary depending on the resolution required.

The SuperSting™ electrical resistivity meter was used to measure resistivity, and the multichannel system automatically determines the electrical configuration and geometric parameters. The device has an internal microprocessor and a switching unit that automatically enables it to record hundreds of resistivity measurements independently. The SuperSting™ resistivity meter also automatically records measurement settings and field setup. The measurement sequence, such as the electric current duration, survey parameter, and configuration type, can be set in the field or prepared beforehand, and uploaded to the microprocessor system (Ghanem *et al*., 2022).

The DC resistivity method is popular due to its simple principles and interpretation. It is employed to determine subsurface resistivity (*rho*). The technique relies on injecting an electrical current into the subsurface via a pair of current electrodes, *A* and *B*, and then measuring the potential difference (ΔV) between two pairs of potential electrodes, *M* and *N*. The current electrodes act as sources *A* and *B* in this process (see Figure 3).

The earth is assumed homogeneous and isotropic, consisting of a single layer with the same resistivity value. Nevertheless, this assumption must be revised since the earth comprises multiple layers with different resistivity values. Therefore, the measurable potential difference in the method only represents an apparent value of various minerals, which results in the apparent resistivity (ρ_a) being calculated by multiplying the geometric factor by the potential difference (ΔV) divided by the current (I) (Reynolds, 1997; Lowrie, 2007). Thus, all quantities can be measured at the ground surface except the resistivity, calculated by Equation (1):

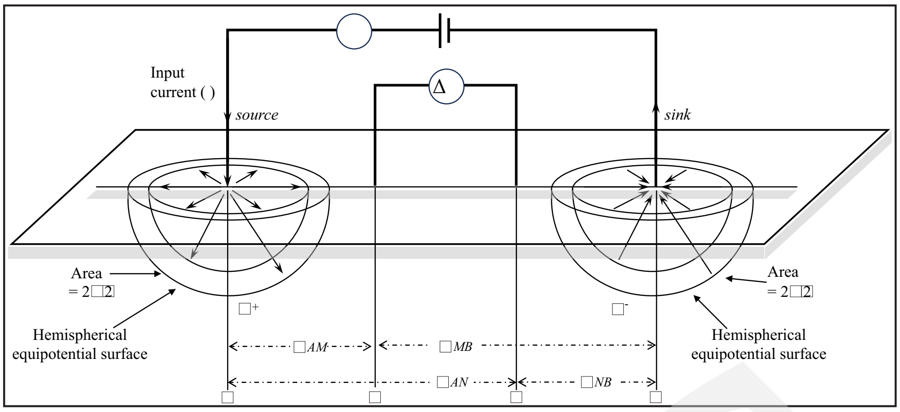

Figure 3. The resistivity measurement employs a standard four-electrode setup comprising two current electrodes, A and B, and an additional pair of potential electrodes labeled *M* and *N*.

$$\rho_a = 2\pi \frac{\Delta V}{I} \left\{ \left(\frac{1}{r_{AM}} - \frac{1}{r_{MB}} \right) - \left(\frac{1}{r_{AN}} - \frac{1}{r_{NB}} \right) \right\}^{-1} \text{ .... (1)}$$

Furthermore, the AGI Earth Imager™ 2D software generated the inverse modeling images. This modeling software created resistivity models by inverting the measured data. Since the site topography is rugged, the resistivity measurements were corrected for topographical variations.

Materials

The resistivity values of different subsurface materials are generally well-defined, which allows for the identification of various layers and structures within the subsurface. In addition, the changes in resistivity values across a fault zone can be used to estimate the location and extent of the fault. The third line (ERT L-3) crosses a hill to intercept the aquifer suspected to flow from a higher surface. The line is characterized by rugged topography, with elevation ranging from 1,141 m asl. to 1198 m asl. and an average slope of 6° to 8°. At 550 m from the first electrode, it intersects with ERT L-1 and ERT L-2.

Figure 4 shows the ERT line survey and the profile elevation. On May 30th, 2022, the first measurement was conducted using the ERT survey with twenty-eight electrodes to investigate the minor buried fault by implementing three lines around the suspected area. Each line is 800 m long and has an electrode spacing of 30 m. The details of the measurement implementation are provided in Table 1. Furthermore, rock specimens were taken in addition to the ERT survey to strengthen the interpretation of geoelectric resistivity measurements (see Figure 5), revealing a tuffaceous rock stratum over the basalt lava.

Figure 5 shows the rock samples collected from the studied area, specifically from the outcrops at SPC-01. These samples possess sandstone, volcanic breccia, basalt lava, and volcanic tuff, which overlays the basalt lava marked by a red dashed line in the stratigraphic profile. The variety of rock types in the samples suggests a dynamic geological history involving sedimentary and volcanic processes. The presence of volcanic tuff above the basalt layer highlights a sequence of volcanic events that followed lava solidification. This samples collection provides crucial data for understanding the geological evolution of the studied area.

Furthermore, Figure 6 presents a comprehensive overview of the morphological and geological characteristics identified in the studied area. It emphasizes critical surface features, including tuff outcrops, river channels, springs, sandstone formations, and alkaline lava exposures. Tuff outcrops indicate layers of volcanic ash deposition, indicating a significant volcanic history in the region. The mapped river channels enhance the understanding of the area drainage patterns and erosion processes. Water springs located along the ERT line imply the existence of groundwa-

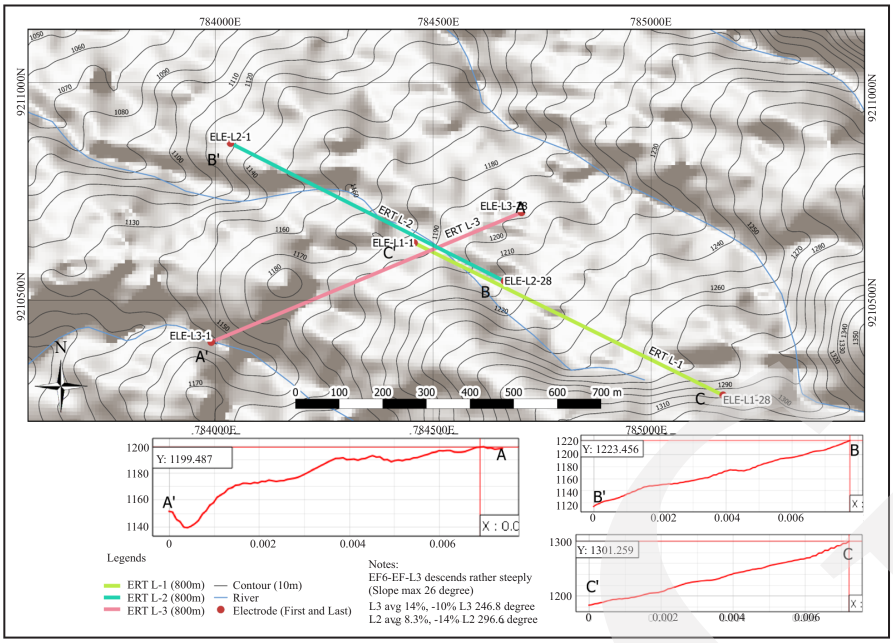

Figure 4. The map depicts the location and orientation of the Electrical Resistivity Tomography lines in the studied area (top). The elevation profiles of each ERT line (A'-A, B'-B, C'-C) include the placement of electrical electrodes (bottom).

Table 1. Information on Deploying the ERT Lines of Resistivity Measurement in the Studied Area (see Figure 4)

ERT Lines		Label, Location (coordinates), and Orientation/elevation (m asl.) of The First and The Last Electrodes			
Label	**Orientation**	**First electrode (ELE-1)**		**Last electrode (ELE-28)**	
ERT L-1	Extending at an azimuth of 296°	ELE-L1-1	785165.65 E, 9210279.52 S (UTM) & about 1300 m asl.	ELE-L1-28	784461.60 E, 9210617.60 S (UTM) & about 1180 m asl.
ERT L-2	Extends from ELE-1 L-2 at an azimuth of 296°	ELE-L2-1	784043.41 E, 9210852.21 S & approx. 1220 m asl.	ELE-L2-28	784678.84 E, 9210531.51 S & around 1130 m asl.
ERL L-3	Intersecting ERT L-1 and ERT L-2	ELE-L3-1	783992.00 E, 9210404.00 S & roughly 1130 m asl.	ELE-L3-28	784700.00 E, 9210711.00 S & approx.1195 m asl.

Table 2. Layer Categories of Resistivity Values

No	Layer category	Resistivity value (Ohm.m)	Colour range in modeling
1	Low resistivity layer	18.9 to 40.5	Dark blue to light blue
2	Medium resistivity layer	40.5 to 186.5	Green blue to yellow
3	High resistivity layer	>200	Yellow to red

ter pathways within the subsurface. Sandstone outcrops reveal sedimentary processes that took place before the volcanic events. Lastly, the alkaline lava exposures indicate historical lava flows, contributing to the region complex stratigraphy. These observations collectively provide essential evidence supporting the geological interpretations outlined in this study.

Result and Analysis

Figure 7 displays the resistivity distribution and topography of each ERT line. Both first (ERT L-1) and second (ERT L-2) profiles follow a downward slope from 1,297 m asl. to 1,190 m asl. with an average slope of approximately 8°. Their resistivity depths reach 155 m from the

Figure 5. The rock specimens obtained from the outcrops found on SPC-01 comprise (a) Sandstone, (b) Volcanic breccia, (c) Basalt lava, and (d) Volcanic tuff (represented by a red dashed line) that overlays the basalt lava.

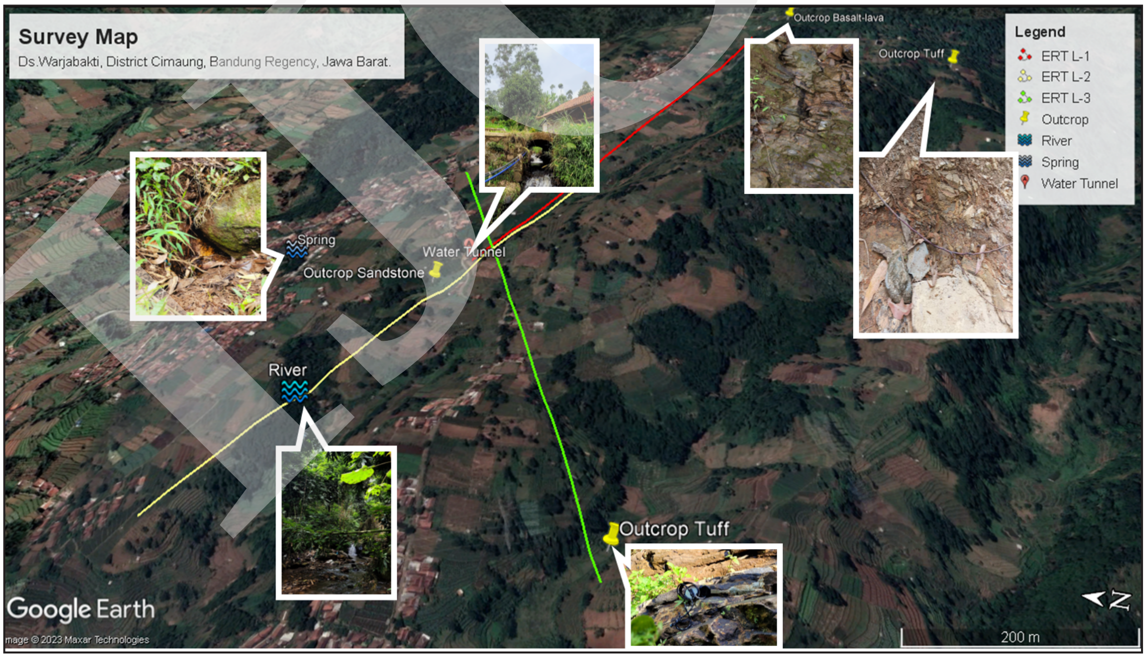

Figure 6. An overview of the morphological and geological characteristics observed on the surface in the studied area, including tuff outcrops, river flows, springs, sandstone outcrops, and alkaline lava outcrops.

surface and 180 m from the ground surface, respectively. The errors of modeling results of ERT L-1 and ERT L-2 are up to 13.23 % and 20.64 %, respectively, with a resistivity range of 18.9 to 400

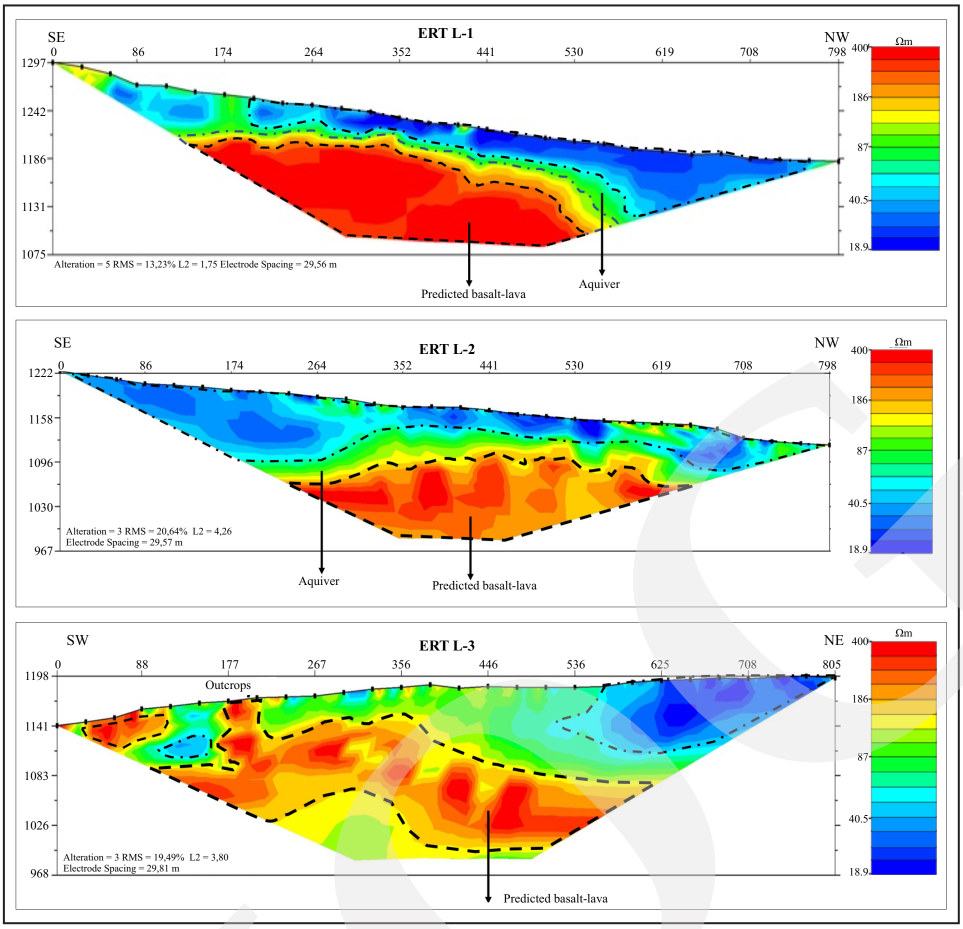

Figure 7. Three ERT profiles from ERT L-1, ERT L-2, and ERT L-3 yielded AGI Earth Imager™ resistivity inversion that varied considerably, with measurement errors ranging from 13.2 to 20.6 %.

Ohm m. The ERT L-3 profile shows a resistivity distribution model with an error of 19.49 %.

The ERT L-1 and ERT L-2 profiles show lines extending to the northwest and intersecting the ERT L-3 profile at the midpoint. Their profiles were then combined to obtain a continuous profile, which follows the survey design in Figure 6 using a roll-along configuration. Thus, the combined cross-section between the two has the length of about 1,400 m. The same colour scale on all profiles provides uniform rock information. The colour discontinuity on the profile indicates the possible location of the minor fault buried.

Discussion

The resistivity values obtained from all ERT line modeling were divided into three categories: low, medium, and high resistivity layers, as presented in Table 2. The low layer is predicted to be an aquifer composed of sandy clay containing groundwater up to 2 m below the surface. The medium resistivity layer likely comprise volcanic tuff and sandstone. It is approximately 20 to 60 m from the surface, because rock resistivity will decrease if rock porosity and saturation increase (Park *et al.*, 2016). The high resistivity layer is found at a depth of approximately 60 m to 155 m from the surface, and is believed to be an aquiclude incapable of storing or transmitting water.

The concatenated cross-sectional results in Figure 8 show that the minor faults may be buried at about 520 m from the first electrode (SE side). This observation was obtained from a discontinuity pattern of resistivity values in the predicted basalt lava layer. Therefore, a minor fault is expected to be buried 160 m below the ground

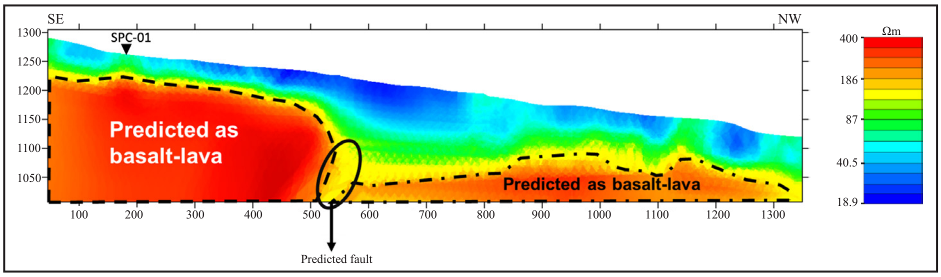

Figure 8. After post-processing, an extension to the resistivity profiles of ERT L-1 and ERT L-2 was made. The profile was 1,400 m long, and reached a depth of approximately 200 m.

surface. This high resistivity layer is predicted to comprise compact basalt lava covered by volcanic tuff, as evidenced by basalt lava outcrops found on SPC-01 at the surface (see Figures 5 and 8). Furthermore, these results are strengthened by the geological map, which confirms that ERT L-1 and ERT L-3 profiles coincide with a suspected fault in the Qmt rock unit area.

Figure 9, a three-dimensional model (visualized from an east–west and a south–north perspective) was constructed to enhance the interpretation based on the intersecting ERT profiles. It demonstrated excellent data quality, as indicated by the well-connected resistivity distribution contours, and interpreted a minor buried fault as a weak zone beneath the soil.

Based on the findings (see Figure 10), the buried minor fault is thought to have a direction from southeast to northwest, with a strike of about N 310°E and a dip of 66°. The identified rock units are believed to include sandy clay in the upper layer, followed by tuff, sandstone, and basalt lava in the lower layer. Thus, the interpretation of resistivity geo-electric data can

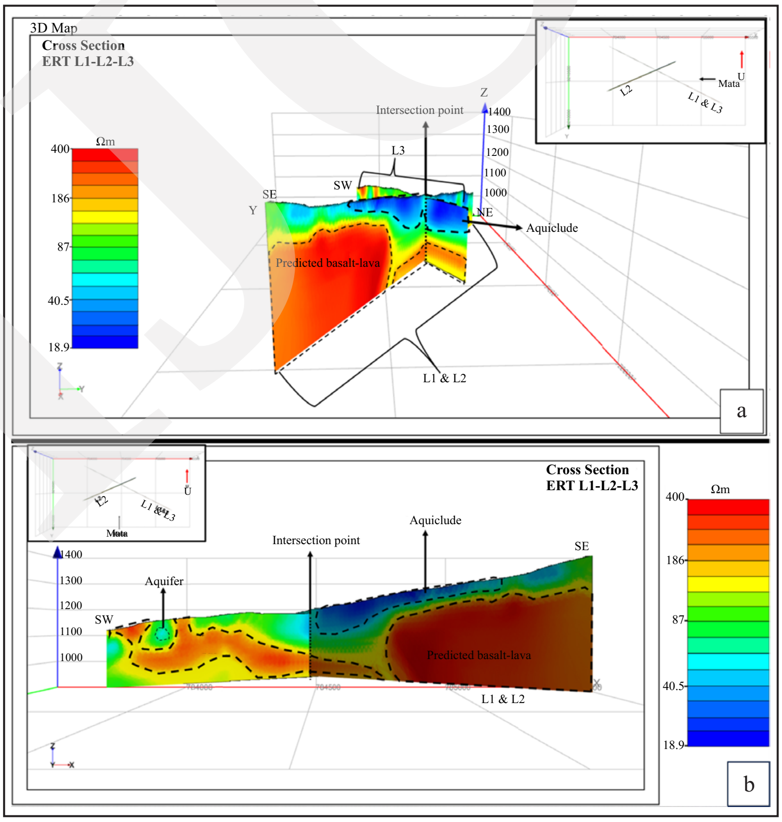

Figure 9. Three-dimensional ERT model: (a) An east-west viewpoint, (b) Another from a south–north viewpoint.

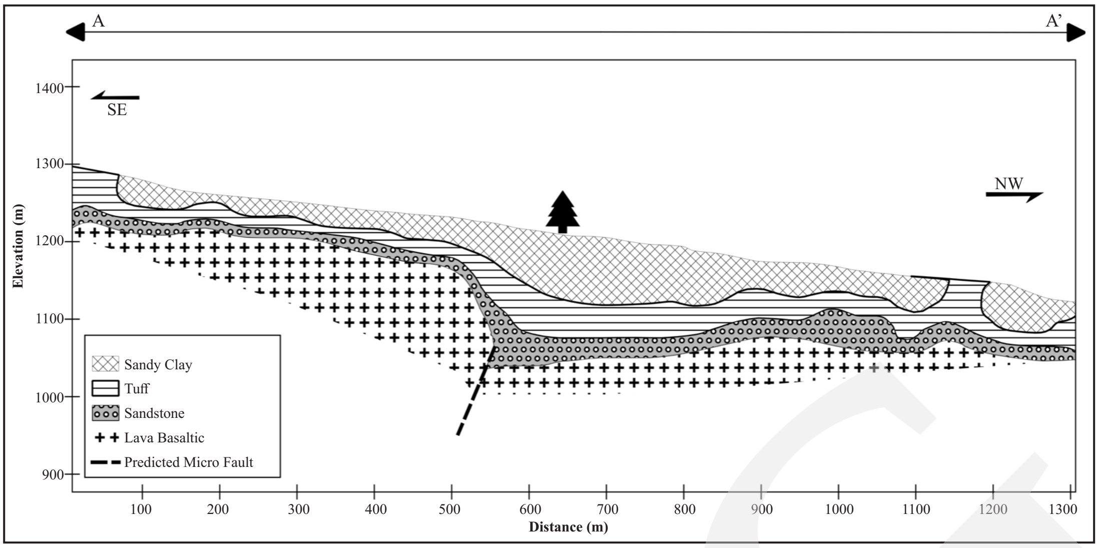

Figure 10. The researched area conceptual model of rock layers is based on the interpretation of resistivity geoelectric data. Suspected rock units include sandy clay, tuff layer, sandstone, and basaltic lava. The discontinuity of the basaltic lava layer at the bottom is attributed to a minor buried fault.

produce a conceptual model of the rock layers in the studied area.

Conclusions

The resistivity measurements obtained from ERT provide valuable information about the subsurface materials, including the presence of fault zones and changes in lithology. This study employed Electrical Resistivity Tomography (ERT) as an effective method to investigate a minor buried fault in the Malabar Mountain. The interconnected cross-sectional analysis suggests the possible existence of buried minor faults at a depth of approximately 160 m, indicated by the observed discontinuity between the assumed layers of basaltic lava (the resistivity of the high layer ranges from 186.5 to 400 Ohm.m). Furthermore, the geological map confirms that ERT L-1 and ERT L-2 intersect with the alleged fault in the Qmt rock unit area. The analysis of the geoelectrical method points out that the buried minor fault may be oriented in a southeast to northwest direction, with a strike of approximately N 310°E and dipping 66°. The buried minor faults might have caused several wells at lower elevations to dry, and the groundwater could have infiltrated the weak zone, causing drought conditions in certain parts of the lower studied area. This discovery of buried minor faults aids in the improvement and completion of the previously established geological map.

Acknowledgments

The successful execution of this research is attributed to the support provided by individuals and organizations outside the authors' team. The authors express gratitude to the Ministry of Education, Culture, Research, and Technology for providing support through the contract number 1949/E2/KM.05.01/2021 and 007/E4.1/AK.04.RA/2021. The authors would also like to thank Dr. Sartono for assisting with geological perspectives. The reviewers are highly appreciated for their constructive comments that improve the quality of the manuscript.

References

Al-Amoush, H. and Rajab, J.A., 2018. The Use of Electrical Resistivity Tomography to Investigate Basaltic Lava Tunnel Based on the Case

Study of Al-Badia Cave in Jordan, *Indonesian Journal on Geoscience*, 5 (2), p.161-177. DOI: 199210.17014/ijog.5.2.161-177.

Alzwar, M., Akbar, N., and Bachri, S., 1992. *Geological Map of Garut and Pameungpeuk Quadrangle, scale 1:100.000.* Geological Research and Development Centre, Bandung

Amukti, R., Alghifari, A.D., Elake, A.Y., and Nendisa, F., 2022. Land Subsidence Investigation in Negeri Sila, Nusalaut Island, Using Resistivity Method, *Indonesian Journal on Geoscience*, 9 (2), p.173-181. DOI: 10.17014/ijog.9.2.173-181.

Binley, A. and Slater, L., 2020. *Resistivity and Induced Polarization: theory and Applications to the Near-Surface Earth.* DOI: 10.1017/9781108685955.

Bogie, I. and Mackenzie, K.M., 1998. The application of a volcanic facies model to an andesitic stratovolcano hosted geothermal system at Wayang Windy, Java, Indonesia. *20th New Zealand Geothermal Workshop*, p.265-270. https://www.geothermal-energy.org/pdf/IGAstandard/NZGW/1998/Bogie.pdf.

Bronto, S., 2006. Stratigrafi gunung api daerah Bandung Selatan, Jawa Barat. *Indonesian Journal on Geoscience*, 1 (2), p.89-101. DOI: 10.17014/ijog.vol1no2.20064.

Dam, M.A.C., Suparan, P., Nossin, Jan J., dan Voskuil, R.P.G.A., 1996. A chronology for geomorphological developments in the greater Bandung area, West-Java, Indonesia. *Journal of Southeast Asian Earth Sciences*, 14 (1-2), p.101-115. DOI: 10.1016/S0743-9547(96)00069-4.

Dam, M.A.C., Suparan, P., Nossin, Jan J., Voskuil, R.P.G.A., and GTL Group, 1996. *Geomorphologic development of the Sunda volcanic complex, West Java. A chronology for geomorphological developments in the greater Bandung area, West Java, Indonesia*, (January 1996).

Drahor, M.G. and Berge, M.A., 2017. Integrated geophysical investigations in a fault zone located on southwestern part of İzmir city, Western Anatolia, Turkey. *Journal of Applied Geophysics*, 136, p.114-133. DOI: 10.1016/j.jappgeo.2016.10.021.

Epting, J., Wüest, A., and Huggenberger, P., 2012. Investigating sediments and rock structures beneath a river using underwater ERT. *Central European Journal of Geosciences*, 4 (1), p. 81–93. https://doi.org/10.2478/s13533-011-0052-0.

Fronzi, D., Mirabella, F., Cardellini, C.,Caliro, S., Palpacelli, S., Cambi, C., Valigi, D., and Tazioli, A., 2021. The role of faults in groundwater circulation before and after seismic events: Insights from tracers, water isotopes and geochemistry. *Water (Switzerland)*, 13 (11). DOI: 10.3390/w13111499.

Galli, P., Bosi., Giocoli, A., and Piscitelli, A., 2006. Late Holocene earthquakes in southern Apennine: Paleoseismology of the Caggiano fault. *International Journal of Earth Sciences*, 95 (5), p. 855-870. DOI: 10.1007/s00531-005-0066-2.

Ghanem, F., Al Amoush, H., and Al-Tarazi, E., 2022. The Use of Electrical Resistivity Tomography and Time Domain Electromagnetic Methods to Investigate the Superficial Deposits at Al al-Bayt University, Jordan as a Case Study. *Indonesian Journal on Geoscience*, 9 (3), p.355-369. DOI: 10.17014/ijog.9.3.355-369.

Griffiths, D.H. and Barker, R.D., 1993. Two-dimensional resistivity imaging and modelling in areas of complex geology. *Journal of Applied Geophysics*, 29 (3-4), p.211-226. DOI: 10.1016/0926-9851(93)90005-J.

Handayani, L., Wardhana, D.D., and Sudrajat, Y., 2012a. Gravity Modeling of Haruman Fault At the East Boundary of Bandung Basin. *Jurnal RISET Geologi dan Pertambangan*, 22 (1), p.23. DOI: 10.14203/risetgeotam2012.v22.55.

Handayani, L., Wardhana, D.D., and Sudrajat, Y., 2012b. Gravity Modeling of Haruman Fault At the East Boundary of Bandung Basin. *Jurnal RISET Geologi dan Pertambangan*, 22 (1), p. 23. https://doi.org/10.14203/risetgeotam2012.v22.55.

Harja, A., Ma'arif, F.R., Nanda, M.D., Duvanovsky, D.A., and Shafa, Z.I., 2021. Studi

Hidrogeofisika Gunung Malabar Sebagai Gunung Tertinggi pada Sistem Hidrologi Cekungan Bandung. *Jurnal Geologi dan Sumberdaya Mineral*, 22 (4), p. 223. DOI: 10.33332/jgsm.geologi.v22i4.654.

Haryanto, I., Sukiyah, E., Ilmi, N.N., Sendjaja, Y.A., and Sunardi, E., 2017. Tectonics Activity and Volcanism Influence to the Garut and Leles Basins Configuration and the Implication on Environmental Geology. *International Journal of Science and Research (IJSR)*, 6 (1), p.2287-2292. DOI: 10.21275/art20164646.

Hendarmawan, 2002. Unconfined aquifer system of volcanics in the northern part of Bandung basin, West Java, Indonesia. *Journal of Geosciences*, 45 (45), p.1-12. https://core.ac.uk/download/pdf/35269175.pdf.

Holmes, J., Chambers, J, and Meldrum, P., 2020. Four-dimensional electrical resistivity tomography for continuous, near-real-time monitoring of a landslide affecting transport infrastructure in British Columbia, Canada. Near Surface Geophysics.

Imposa, S., De Guidi, G. , Grassi, S., Scudero, S., Barreca, G., Patti, G., and Boso, D., 2015. Applying geophysical techniques to investigate a segment of a creeping fault in the urban area of San Gregorio di Catania, southern flank of Mount Etna (Sicily - Italy). *Journal of Applied Geophysics*, 123, p.153-163. DOI: 10.1016/j.jappgeo.2015.10.008.

Jacob, R.W., Byler, J.B., and Gray, M.B., 2013. Integrated geophysical investigation of the St. James Fault Complex: A case study. *Geophysics*, 78 (5). DOI: 10.1190/GEO2012-0426.1.

Lowrie, W., 2007. *Fundamentals of Geophysics, Second Edition*, Cambridge University Press.

Marc, V., Bertrand, C., Male, J.P., Carry, N., Simler, R., and Cervi, F., 2017. Groundwater-Surface waters interactions at slope and catchment scales: implications for landsliding in clay-rich slopes. *Hydrological Processes*, 31 (2), p.364-381. DOI: 10.1002/hyp.11030.

Nurpadillah, S., Cahyadi, W.A., Mukhtar, H., and Susanto, K., 2024. Optimizing Current Injection Technique for Enhancing Resistivity Method. *International Journal of Electrical and Electronics Research*, 12 (1), p.99-110. DOI: 10.37391/IJEER.120115.

Park, S.G., Shin, S.W., Lee, D.K., Kim, C.R., and Son, J.S., 2016. Relationship between electrical resistivity and physical properties of rocks. *22nd European Meeting of Environmental and Engineering Geophysics, Near Surface Geoscience*. DOI: 10.3997/2214-4609.201602101.

Pratama, A., Irawan, D.E., Susanto, A., and Ardi, R.D.W.,2016. Influence of Lithology and Slope Gradient to Infiltration of the Mount Malabar, West Java. *IOP Conference Series: Earth and Environmental Science*, 29 (1), p.1-7. DOI: 10.1088/1755-1315/29/1/012025.

Qiang S, Shi X, and Kang X., 2022. Optimized arrays for electrical resistivity tomography survey using Bayesian experimental design. *Geophysics,* 87 (4):E189-E203.

Rey, J., Martínez, J., Mendoza, R., Sandoval, S., Tarasov, V., Kaminsky, A., Hidalgo, M.C., and Morales, K., 2020. Geophysical characterization of aquifers in southeast spain using ERT, TDEM, and vertical seismic reflection. *Applied Sciences*, 10 (20), p.1-16. DOI: 10.3390/app10207365

Reynolds, A., 1997. *An introduction to applied and environmental geophysics*, 796pp. DOI: 10.1071/pvv2011n155other.

Saputra, D.R., Yudono, A.R.A., and Partoyo, 2020. Assessment of the groundwater recharge potential areas using GIS in Kajor Kulon Hamlet, Selopamioro, Imogiri, Bantul, Yogyakarta. *Jurnal Geografi Lingkungan Tropik*, 4 (2). DOI: 10.7454/ jglitrop.v4i2.89.

Torz, H., Storz, W., and Jacobs, F., 2000. Electrical resistivity tomography to investigate geological structures of the earth's upper crust. *Geophysical Prospecting*, 48 (3), p.455-471. DOI: 10.1046/j.1365-2478.2000.00196.x.

Sudarman, S., Pujianto, R., and Budiarjo, B., 2006. The Gunung Wayangwindu Geothermal Area In West Java. *Proceedings of Indonesian Petroleum Association,* 15th Annual Convention.

Suhari, S. and Siebenhüner, M., 1993. Environmental geology for land use and regional planning in the Bandung Basin, West Java, Indonesia. *Journal of Southeast Asian Earth Sciences*, 8 (1-4), p.557-566. DOI: 10.1016/0743-9547(93)90053-R.

Sulaksana, N., Iskandarsyah, T.Y.W.M., Rifai,A., Rendra, P.P.R., and Sulastri, M., 2019. Prospective zone area for agriculture and residential based on geological disaster potentials in south Bandung region. *Journal of Geological Science and Applied Geology*, 3, p.26-37. http://jurnal.unpad.ac.id/gsag/article/viewFile/ 21366/10585.

Susanto, K., Azzam, M.Z., Syarafina, Z.N., Kirana, K.H., Dharmawan, I.A., and Harja, A., 2023. Investigasi Lapisan Batuan Kawasan Pendidikan Universitas Padjadjaran Jatinangor Bagian Utara Berdasarkan Electrical Resistivity Tomography (ERT). *Bulletin of Scientific Contribution: Geology*, 21, p.61-70.